J|A|C|S
COMMUNICATIONS

Published on Web 05/15/2007

Probing a Fibrillation Nucleus Directly by Deep Ultraviolet Raman Spectroscopy

Victor Shashilov, Ming Xu, Vladimir V. Ermolenkov, Laura Fredriksen, and Igor K. Lednev*

Department of Chemistry, University at Albany, State University of New York, 1400 Washington Avenue, Albany, New York 12222

Received January 3, 2007; E-mail: lednev@albany.edu

Understanding the biochemical mechanism of amyloid fibrillation is one of the most intriguing and pressing problems in modern biology and medicine.[1] On the basis of kinetic studies of fibril formation, several hypothetical mechanisms for fibrillation have been proposed recently.[2] It is well accepted now that the fibrillation starts with a thermodynamically unfavorable nucleation step followed by a rapid elongation of fibrils.[3] The understanding of the nucleation mechanism is crucial for developing inhibitors for a limiting stage of the pathological process. So far, the proposed nucleation models[4−6] have been verified by correlation of the fibrillation lag-time or the rate of fibril accumulation with protein concentrations and other experimental conditions. According to the thermodynamic nucleus model for homogeneous nucleation, the nucleus is defined as a metastable species (free energy minimum),[4,5] the formation of which determines the lag-phase of fibrillation.

We report here on the application of deep UV resonance Raman (DUVRR) spectroscopy combined with advanced statistical analysis including 2D-correlation spectroscopy, independent component analysis (ICA), and pure variable methods, to study nucleus formation during the fibrillation of hen egg white lysozyme, a well studied model of amyloidogenic proteins. Over the course of fibrillation, the soluble portion of the sample, as well as those insoluble aggregates separated by ultracentrifugation, were analyzed separately. Although the supernatant contained no fibrils, as evidenced by dynamic light scattering, the solution was a potent initiator of fibrillation, eliminating the fibrillation lag-phase on addition to lysozyme. The application of advanced statistical analysis to the Raman spectroscopic data yielded spectroscopic signatures of a partially unfolded intermediate and newly formed β-sheet and enabled determination of species-specific kinetic profiles in the early stages of fibril formation and evaluation of the rate constants for corresponding process.

Fibrils were prepared by incubating a solution of lysozyme at pH 2.0 and 65 °C for various times. Three sets of spectra (over 20 spectra each) were obtained at three different initial lysozyme concentrations, 70, 14, and 1.4 mg/mL. The time dependent lysozyme DUVRR spectra are shown in Figure 1. The spectra exhibit pronounced amide bands which report on the protein secondary structure.[7] In particular, the $C_\alpha-H$ bending band is strong in deep UVRR spectra of random coil and β-sheet, where the adjacent $C_\alpha-H$ and N−H bending vibrations are coupled, and weak for peptides in the α-helical form.[7] The frequency of the $C_\alpha-H$ bending mode is different for β-sheet (~1396 cm^{-1}) and random coil (~1387 cm^{-1}) conformations. This band is especially sensitive to secondary structural transformations of proteins. The $C_\alpha-H$ bending band intensity increased with lysozyme incubation time, indicating the melting of the α-helix and the formation of the β-sheet and random coil. The evident decrease in the 1000-cm^{-1} phenylalanine band intensity during the incubation corresponds to the tertiary structural changes of lysozyme.[8] At the early stages of fibrillation, the melting of native lysozyme and the formation of a partially unfolded intermediate has been reported[8] to be accompanied by a small β-sheet contribution. Classical factor analysis suggested the existence of only two principle components, indicating that the formation of β-sheet and the unfolding of native lysozyme are highly correlated.[9] We utilized 2D correlation Raman spectroscopy to distinguish these correlated processes and establish their sequential order. Synchronous $\Phi(\nu_1,\nu_2)$ and asynchronous $\Psi(\nu_1,\nu_2)$ 2D-Raman spectra were calculated following Noda's approach:[10]

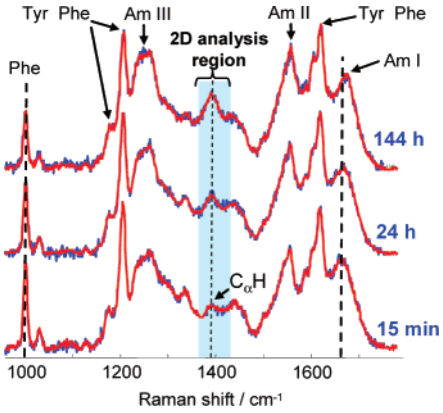

Figure 1. Experimental (blue) and modeled (red) DUVRR spectra of lysozyme incubated for various times. The nature of Raman bands is described in Supporting Information.

$$\Phi(\nu_1,\nu_2)+i\Psi(\nu_1,\nu_2)=\frac{1}{\pi(T_{max}-T_{min})}\times\int_0^\infty \tilde{Y}_1(\omega)\,\tilde{Y}_2^*(\omega)\,d\omega \quad (1)$$

where $\tilde{Y}_1(\omega)$ and $\tilde{Y}_2^*(\omega)$ were calculated based on experimental spectral intensities $\tilde{y}(\nu,t)$ for all wavenumbers ν and incubation times t[10].

The asynchronous 2D-Raman correlation map is shown in Figure 2 for the $C_\alpha-H$ bending region. The peak and the valley centered at 1385 and 1400 cm^{-1}, respectively, illustrated (i) that changes in random coil and β-sheet spectral regions occurred asynchronously and (ii) that the formation of the β-sheet was delayed with respect to the formation of the random coil. These data can be used to distinguish between two alternative mechanisms of β-sheet formation. In a parallel process mechanism, random coil and β-sheet are produced directly from the native protein and should be completely correlated. In a step-by-step mechanism, β-sheet develops from the partially unfolded intermediate (Scheme 1). In the latter case, the formation of β-sheet and the partially unfolded intermediate could correlate, but only partially. Consequently, the step-by-step mechanism proposed by Dobson and co-workers[11] (Scheme 1) was in complete agreement with our analysis above. Following the

10.1021/ja070038c CCC: $37.00

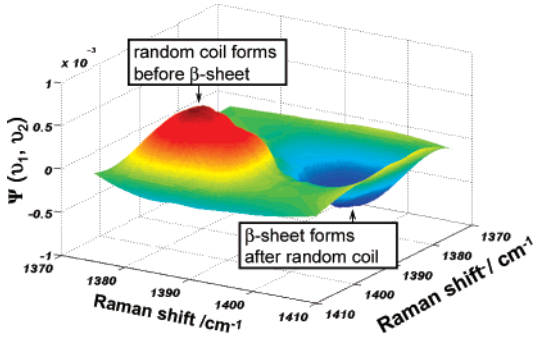

Figure 2. Asynchronous 2D correlation spectrum of the $C_\alpha H$ region of lysozyme DUVRR spectra. Two opposite-sign areas at 1387/1396 cm^{-1} and 1396/1387 cm^{-1} indicate asynchronous formation of random coil and β-sheet; valley at 1396/1387 cm^{-1} shows that β-sheet appeared after random coil. This result unambiguously indicated that the appearance of β-sheet and random coil at the early stages of lysozyme fibrillation was incompletely correlated.

Scheme 1. Mechanism of Lysozyme Fibril Formation[a]

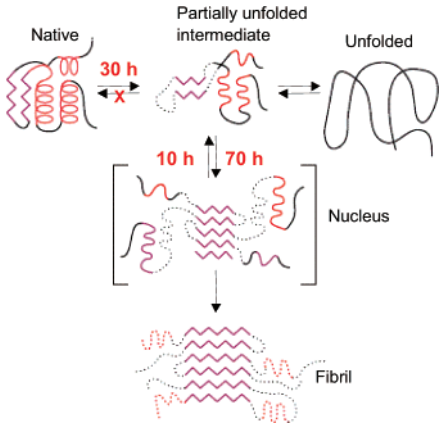

[a] Adopted from Booth et al.[11] Blue is β-sheet, red is helical structure, dotted line is undefined structure.

proposed step-by-step mechanism, the newly formed β-sheet in the solution part of the incubated samples could be assigned to the fibrillation nucleus. To further support this assignment, the supernatant of a lysozyme sample incubated for 48 h was used for seeding the fibrillation of fresh lysozyme. The seeding was successful and the fibrillation lag-phase was eliminated.

Here we report on the first application of joint diagonalization Jade,[12] SOBI in the Fourier space data,[13] and SEONS[14] ICA algorithms for the analysis of protein structural evolution. The ICA methods were used to resolve sets of DUVRR spectra into pure spectra of native protein, partially unfolded intermediate, and nucleus β-sheet. It is noteworthy that the DUVRR spectroscopic signature of the β-sheet was very close to the spectrum of lysozyme fibrils (see Figure S1, Supporting Information), and all three methods gave similar results.

The newly formed β-sheet may only be a portion of the nucleus, leaving the rest of the protein unchanged. Similar to differential spectroscopy, our method specifically probes and characterizes protein structural transformations by eliminating the contribution of unchanged parts.

All experimental Raman spectra were fitted with three pure component spectra, that is, the spectra of the nucleus β-sheet and partially unfolded intermediate calculated by ICA, and the experimental spectrum of native lysozyme. A mixed soft−hard modeling approach[15] provided the refined DUVRR spectra of β-sheet and partially unfolded intermediate, kinetic profiles for all three species, and the characteristic times for each step of lysozyme transformation (Table 1). Namely, the algorithm was used to (i) calculate kinetic profiles by guessing the initial characteristic times, (ii) fit experimental spectra using the kinetics profiles and pure components spectra, and (iii) iterate over the characteristic time constants until the best fitting is achieved. The independence of the characteristic times on protein concentration indicated that the early stages of lysozyme fibrillation, irreversible partial unfolding and nucleus β-sheet formation, were intramolecular processes.

Table 1. Characteristic Times for Transformations: Native → Partial Intermediate (τ_1), Partial Intermediate → Nucleus (τ_2), and Nucleus → Partial Intermediate (τ_{-2})

concentration mg/mL	characteristic time, hours		
	τ_1	τ_2	τ_{-2}
70	30 ± 2	70 ± 20	15 ± 5
14	30 ± 2	70 ± 10	12 ± 3
1.4	30 ± 2	74 ± 16	14 ± 5

This study showed that deep UV resonance Raman spectroscopy combined with 2D-correlation spectroscopy, independent component analysis, and advanced alternating least-squares modeling is a powerful tool for the quantitative characterization of protein structural rearrangements and could be used for various protein folding problems.

Acknowledgment. We are grateful to Dr. I. Noda and Profs. J. Welch, R. Zitomer, and B. Szaro for valuable advice.

Supporting Information Available: Details on sample preparation and data treatment, the synchronous 2D-Raman correlation map, and resolved DUVRR spectrum of nucleus β-sheet. This material is available free of charge via the Internet at http://pubs.acs.org.

References

(1) Chiti, F.; Dobson, C. M. *Ann. Rev. Biochem.* **2006**, *75*, 333−366.
(2) Ohnishia, S.; Takano, K. *Cell. Mol. Life Sci.* **2004**, *61*, 511−524.
(3) Sabaté, R.; Gallardo, M.; Estelrich, J. *Int. J. Biol. Macromol.* **2005**, *35*, 9−13.
(4) Crick, S. L.; Jayaraman, M.; Frieden, C.; Wetzel, R.; Pappu, R. V. *Proc. Natl. Acad. Sci. U.S.A.* **2006**, *103*, 16764−16769.
(5) Ferrone, F. *Meth. Enzymol.* **1999**, *309*, 256−274.
(6) Librizzi, F.; Rischel, C. *Protein Sci.* **2005**, *14*, 3129−3134.
(7) Asher, S. A. In *Handbook of Vibrational Spectroscopy*; John Wiley & Sons, Ltd.: Chichester, U.K., 2002; pp 557−571.
(8) Xu, M.; Ermolenkov, V. V.; He, W.; Uversky, V. N.; Fredriksen, L.; Lednev, I. K. *Biopolymers* **2005**, *79*, 58−61.
(9) Shashilov, V. A.; Xu, M.; Ermolenkov, V. V.; Lednev, I. K. *J. Quant. Spectrosc. Radiat. Transfer* **2006**, *102*, 46−61.
(10) Noda, I.; Ozaki, Y. *Two-Dimensional Correlation Spectroscopy: Applications in Vibrational and Optical Spectroscopy;* John Wiley & Sons: Hoboken, NJ, 2004.
(11) Booth, D. R.; Sunde, M.; Bellotti, V.; Robinson, C. V.; Hutchinson, W. L.; Fraser, P. E.; Hawkins, P. N.; Dobson, C. M.; Radford, S. E.; Blake, C. C. F.; Pepys, M. B. *Nature (London)* **1997**, *385*, 787−793.
(12) Cardoso, J.-F. *Neural Comp.* **1999**, *11*, 157−192.
(13) Nuzillard, D.; Nuzillard, J.-M. *Signal Process.* **2003**, *83*, 627−631.
(14) Choi, S.; Cichocki, A.; Belouchrani, A. *J. VLSI Signal Process.* **2002**, *32*, 93−104.
(15) Amigoa, J. M.; de Juan, A.; Coello, J.; Maspocha, S. *Anal. Chim. Acta* **2006**, *567*, 245−254.

JA070038C